

Design, Characterization and Investigation of Heavy Metal Ions Removal by New Cellulose-Ether Based adsorbent

C. Zannagui^a, H. Amhamdi^{a*}, S. El Barkany^{b*}, I. Jilal^b, O. Sundman^c, A. Salhi^a, S. Chaouf^d, M. Abou-Salama^b, A. El Idrissi^d, M. Zaghrioui^e

^aUnit of Applied Chemistry, Faculty of Sciences and Techniques, Abdelmalek Essaadi University, 32 003 Al Hoceima, Morocco

^bLaboratory of Molecular Chemistry, Materials and Environment (LCM2E), Multidisciplinary Faculty of Nador, Department of Chemistry, Mohamed first University, 60700 Nador, Morocco

^cDepartment of Chemistry, Umeå University, Sweden

^dLaboratory of applied chemistry and environmental (LCAE-URAC18), Faculty of Sciences of Oujda, Mohamed1st University, 60000 Oujda-Morocco

^eLaboratoire GREMAN CNRS-UMR 7347 IUT-BLOIS, France

Abstract

The present investigation deals with the elaboration in homogenous conditions of new cross-linked, hydroxyl cellulose (HEC) based material. Further, its application as a new eco-friendly low-cost efficient adsorbent of hazardous metal ions from an aquatic environment is treated. In this respect, the functionalization of HEC has been carried out using EDTA as a cross-linking agent exploiting its high capacity to chelate heavy metal ions in aqueous solutions. The proposed structure of the new crosslinked material (HECD) was investigated using structural analyses (FTIR-ATR vibrational spectroscopy and CP/MAS 13C NMR Spectroscopy). Also, the thermal and crystalline behaviours of unmodified and modified HEC were studied using thermogravimetric (TG and DTG) and DRX patterns. In addition, SEM images were recorded to demonstrate the changes expected at the morphological and textural level. Furthermore, the adsorption capacity of Pb (II), Cu (II), Cd (II) and Zn (II) ions from aqueous solutions by HECD was investigated using batch technique and optimized according to metal concentration, pH, contact time, ionic selectivity and regenerability. Thus, to examine the mechanism of adsorption, the experimental data is fitted to kinetic, isothermal, and thermodynamic modelling.

* Corresponding author:
el.barkany011@gmail.com;

Received 16 Dec 2019,

Revised 08 march 2020,

Accepted 12 March 2020

Keywords: Hazardous Metal ions, Hydroxyethyl cellulose-EDTA, Adsorption Capacity, eco-friendly and low-cost adsorbent

1. Introduction

Water is an indispensable substance in all natural and anthropogenic activities, and among the most recommended research are those intended for the removal of micropollutants from the aquatic medium, where the increased awareness of these hazardous substance toxicity has led to strict regulations for its elimination. In particular, toxic metal ions such as Pb (II), Cu (II), Cd (II) and Zn (II) are classified among the most dangerous particles even at low concentration ranges [1, 2]. Indeed, the heavy metal ions are not degradable to harmless matter during the metabolism, they easily tend to accumulate in the vital organs of humans and animals through their transformation in trophic chains, where several studies have shown their adverse effects on human physiology and other biological systems giving rise to serious diseases such as developmental delay [3], several types of cancers [4], kidney damage [5], etc. Heavy metals are released into the environment through various anthropogenic activities where can be readily penetrated into water supplies, and therefore, the rejection regulations are more stringent and emphasize the treatment of contaminated water within industries is required prior to discharge. Conventional methods include chemical precipitation [6], membrane separation [7], flocculation [8-10] and ion exchange [11, 12], are widely used for the removal of heavy metal ions from industrial effluents and electrolysis. However, the majority of these techniques is frequently costly, less adapted or ineffective. Nevertheless, each of these methods has specific advantages and disadvantages, where the adsorption technique is one of the most popular and effective methods for the removal of heavy metals [13]. Recently, modified biopolymers intended for adsorption received a lot of attention because they are environmentally friendly, biodegradable and less toxic and above all, easy processing and many functional groups sensitive to chemical reactions. However, to reduce all these problems related to the environment and to operational costs, the search for alternative and eco-friendly adsorbents has intensified in recent years. Several biomass and biopolymer-based adsorbents reported in the literature include fruit peels (orange, hazelnut, Guar gum, etc.) [2, 14-17], Natural bentonite [18, 19], polysaccharides based polymers (chitosan, alginate, etc.) [20-22] have been studied for the removal of heavy metals. Yet, these materials usually have low adsorption capacities in the received forms and improving their performance by chemical modification is necessary [23-25]. Cellulose is the most abundant linear polysaccharide biopolymer with long chains that consist of α -D-glucopyranose units linked by α -1,4 glycosidic linkages [26], it is well used in many applications as a building material, mainly in the form of wood and textile fibers or in the form of paper, but also used as a derivative in many industrial areas and domestic life [27]. Although cellulose is a linear polymer contains two types of hydroxyl groups, primary hydroxyl ($-\text{CH}_2\text{OH}$) at C-6 and secondary hydroxyl groups ($-\text{OH}$) at C-3 and C-4, which are less reactive than the primary hydroxyl. The insolubility in most common solvents remains to be the challenges in processing cellulose for effective utilization. Nevertheless, cellulose can be directly modified through the reaction of functional groups with hydroxyl groups on the cellulose surface and several works based on cellulose chemical modifications have been carried out to enable the adsorption of organic, inorganic, and heavy metal pollutants from aqueous solutions [27-31]. Hydroxyethyl cellulose (HEC) is a commercially important cellulose ether derivative used extensively in chemical industry and common life as a stabilizer [32], emulsifier [33], pharmaceutical, cosmetic and thickener or coating [34, 35], which have been developed basically to overcome the limitations of cellulose solubility and properties, it can be prepared by the etherification reaction of cellulose with chlorohydrin in NaOH/Urea aqueous solution [36]. However, HEC was selected among the cellulosic derivatives for its better solubility in conventional solvents and its homogeneous chemical modification giving a number of additional advantages, including ease of preparation and production of highly substituted derivatives, selectivity and homogeneity in the substitution pattern. In this study, modified hydroxyethyl cellulose was synthesized by incorporation of EDTA groups into the polysaccharide chain through a crosslinking reaction. Ethylenediaminetetraacetic acid dianhydride (EDTAD) is an active agent presenting two

anhydride groups easily reacting with hydroxyl groups of HEC. The new crosslinked material (HECD) was analyzed by FTIR-ATR, SEM, RMN ^{13}C solid-state and thermogravimetry analysis (TG and DTG). Present work aimed at metal ions uptake under optimum conditions using HECD material and the experimental data were fitted to kinetic, isotherms and thermodynamic modelling in order to examine the mechanism of adsorption. This investigation also dealt with selectivity studies and reproducible performance of regenerated material. In our knowledge, this new adsorbent has never been discussed in the literature either on the synthesis side or on the application side, where HECD constitute a new candidate promising to be an acceptable adsorbent at the industrial level, especially with its characteristics responding to environmental criteria and its high efficiency with short contact times.

2. Material and Methods

2.1. Material

Hydroxyethyl cellulose (HEC, DS = 1.5) powder was purchased from HIMEDIA Company, pyridine and acetic anhydride, were obtained from Sigma Aldrich. Triethylamine (TEA), 4-diméthylaminopyridine (DMAP) and dimethylformamide (DMF) were purchased from Sigma-Aldrich Company, ethanol and KOH were obtained from Merck. All other chemicals were used without further purification and were of analytical grade. The stock solution of metals was prepared with deionized water, and HCl (0.1N) and NaOH (0.1N) aqueous solutions were used for pH adjustment.

2.2. Methods

The chemical structure was evaluated using the vibration spectroscopy technique (FTIR-ATR), the spectra were performed on Shimadzu FTIR-8400S FTIR spectrometer using the KBr pellets of finely ground with 2% of the sample at a resolution of 2 cm^{-1} from 4000 to 400 cm^{-1} and an average of 40 scans were taken for each sample. Solid-state CP/MAS ^{13}C NMR spectrum was attained at ambient temperature (100 MHz, NS 5000, acquisition time 0.032 s, delay time 2 s, proton 90° , pulse time 4.85 μs) using Bruker DRX-400 machine. The number of scans was typically 1800. The crystallinity of each sample was studied by X-ray diffraction technique and the patterns were recorded on an X-ray Diffractometer EQUINOX 2000 using copper radiation $\text{CuK}\alpha$ ($\lambda = 1.5418 \text{ \AA}$), at an accelerating voltage of 40 kV and an operating current of 30 mA in the range of 2θ (05° - 60°), 0.25 g of each sample was pressed under 50 MPa to form the pellets of an average of 25 mm in diameter. SEM images were obtained on a FEI-Quanta 200. The thermal stability and the mass loss determinations were performed under air in a platinum crucible on a Shimadzu DTG-60 simultaneous DTA-TG apparatus at a heating rate of 10 $^\circ\text{C min}^{-1}$ under nitrogen at a flow rate of 50 mL/min. All metal ion concentrations were determined by atomic absorption measurements were performed by Spectra Varian A.A. 400 spectrophotometer.

2.3. Synthesis of EDTA dianhydride (EDTAD)

Ethylenediaminetetraacetic acid (15g) was suspended in anhydrous pyridine (27 mL) under strong stirring, and then acetic anhydride (21 mL) was added drop-wise into the mixture. The reaction was maintained at 65 $^\circ\text{C}$ under stirring for 22 h. A solid phase (EDTAD) obtained was filtered, washed with acetic anhydride and diethyl ether and stored in a desiccator [30].

2.4. Synthesis of crosslinked HEC (HECD)

The preparation of crosslinked HEC was performed in a homogeneous medium using 4-Dimethylamino-pyridine (DMAP) as esterification catalysts. 2g of Hydroxyethyl cellulose (8.77 mmol) was dissolved in DMF (40

mL) and was drop-wise added to the solution of EDTAD already dissolved in DMF under stirring at 70 °C (26.31 mmol). DMAP (30 mmol) and TEA (4.38 mmol) were added to the mixture and the stirring reaction was kept for 1h at 70 °C. The modified material (HECD) was separated by filtration, treated with saturated sodium bicarbonate solution, washed with deionized water, ethanol 95%, acetone and dried in an oven at 60 °C for 8h.

2.5. Determination of total amount of crosslinker and grafted in the HECD

The degree of substitution (DS), the percentage of crosslinked-EDTAD (%Cr) and that of grafted-EDTAD (%Gr) were determined by two different titration methods. Firstly, Ester content in the product was calculated according to Tanghe et al. method [37], where 200 mg of acidified HECD was weighed accurately and 30 mL of aqueous NaOH (0.1 N) then added, and the mixture was heated at 50 °C for 3 h for hydrolysis of ester linkages between EDTA and cellulose. The mixture was cooled to room temperature, and the NaOH consumed for ester hydrolysis was determined by the back-titration with HCl (0.1 N) aqueous solution using phenolphthalein as an indicator for the titration. Total ester linkages (E) were calculated in mmol.g⁻¹. In the second titration, the tetrasodium EDTA, which was produced by the alkaline hydrolysis, was titrated with a standard solution of CaCl₂. 0.5 g of sample was added to 20 ml of 75% aqueous ethanol into a 250 ml flask and heated for 30 min at 60 °C. Then 20 ml of 0.5 M NaOH solution was added and again heated at 60 °C for 15 min. The same procedure was also carried out for a control system (not containing HECD material). The mixtures were stoppered and kept at room temperature for 72 h. The solutions were filtered, transferred to a 100 ml volumetric flask and filled up to the mark with distilled water then 10 ml was transferred to Erlenmeyer's flasks and 10 ml of ammoniacal buffer pH ~ 10 was added with Eriochrome Black as an indicator. The samples were then titrated with a standard solution of 0.01 M CaCl₂ to the endpoint. This titration allowed to calculate the weight of EDTA crosslinked and grafted (mmol.g⁻¹) in the polymeric network using eq.1 and eq. 2:

$$\%Cr = \left[\left(\frac{E_{EDTA}}{mm_{EDTA}} - 1 \right) \right] \times 100 \quad eq.1$$

$$\%Gr = 100 - \%Cr \quad eq.2$$

2.6. Batch experiments

The adsorption capacity of HECD to removal Pb(II), Cu(II), Cd(II) and Zn(II) from aqueous solutions, was studied using 10 mg of the adsorbent in 10 mL of metal ion aqueous solution. The metal ion concentrations were varied from 10 to 500 mg. L⁻¹ and the effect of pH was studied in the range of 1 to 7. The kinetic study was carried out by varying contact time from 5 to 60 min and the agitation was conducted under magnetic stirring at room temperature (25 °C). At the equilibrium, the solid phase was separated by centrifugation and the supernatant was recovered. The residual metal concentration was measured by flame atomic absorption (*ThermoScientific iCE3000, Type iCE3500AA System*). The adsorption capacity was expressed by the amount of metal ions adsorbed per unit mass of modified cellulose (mg.g⁻¹) using the following equations (eq. 3 and 4):

$$q_M = (C_0 - C_e) \times \frac{V}{M} \quad (eq.3)$$

$$q_n = \frac{q_M}{M_w} \quad (eq.4)$$

Where q_M and q_n are the mass (mg.g⁻¹) and the amount (mmol.g⁻¹) of the metal ion adsorbed, respectively. C₀ and C_e are the initial and equilibrium concentrations (mg. L⁻¹), respectively. M is the weight of the adsorbent (mg), V is the volume of the solution (L) and M_w is the molar mass of the ion in question.

3. Results and discussion

3.1. Synthesis and characterization of HECD

3.1.1. Route synthesis

In the present study, Modified hydroxyethyl cellulose (HECD) was synthesized by crosslinking reaction through esterification, DMAP was used as a catalyst. To achieve homogeneous reaction HEC was dissolved in DMF and was drop-wise added to EDTAD solution, DMAP was added in excess to the solution to achieve a high degree of crosslinking [38]. During the reaction, a decrease in viscosity of the system was observed. Fig. 1 shows the schematic illustration of synthesizing of novel HECD. HEC is known as a water-soluble biopolymer and its crosslinking resulted in a derivative insoluble in hot and cold water, DMSO, ethanol and methanol and provided the basis for its use in the removal of metal ions from aqueous solution. During the reaction, a decrease in viscosity of the system was observed. In order to eliminate unreacted EDTA and to liberate carboxylate functions, the carboxyl groups of EDTA were converted to sodium carboxylate groups by dispersing the product in aqueous NaHCO_3 . The percentages of crosslinked-EDTAD and grafted-EDTAD and DS were calculated, which given; $\text{DS} = 1.4$, $\% \text{Cr} = 73.85 \%$ and $\text{Gr} = 26.15 \%$.

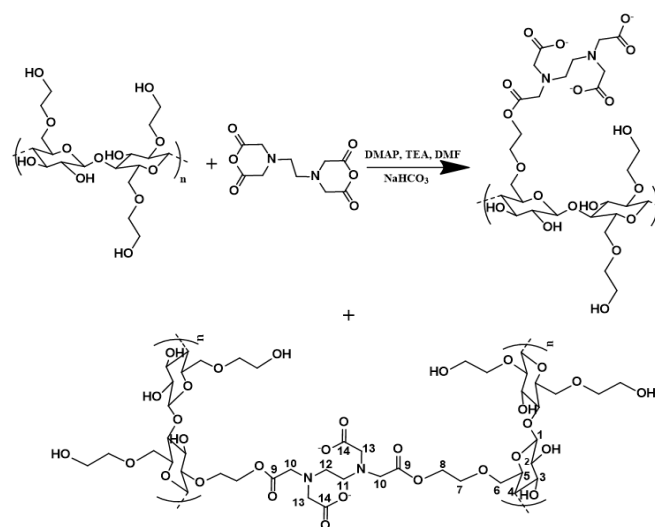


Figure 1: The synthesis route of HECD

3.1.2. FTIR-ATR spectroscopic analysis

Following the crosslinking esterification reaction of HEC with EDTAD, Fig.2 shows the FT-IR spectra of unmodified HEC, EDTA and HECD. The spectrum of HEC shows a broad absorption band at 3446 cm^{-1} due to O–H stretching vibrations and the O–H bending located at 1458 cm^{-1} [39]. The C–H stretching and bending vibrations are designated by bands at 2925 cm^{-1} , 2880 cm^{-1} and 1429 cm^{-1} [31]. On the other hand, The C–O–C stretching vibration is present at 1126 cm^{-1} and the group of bands at 1057.2 and 1020 cm^{-1} can be assigned to C–O stretching vibrations. The obtained product (HECD) showed several new absorption bands in the FTIR spectrum. The new broad absorption band at 1746 cm^{-1} was attributed to the C=O stretching vibration of the ester group resulting from crosslinking of EDTA. Whereas, ester signal of HECD was shifted towards relatively higher absorption (intense peak) as expected due to cross-linking by ester formation as well [40]. The absorption appearing at 1594 cm^{-1} was assigned to the C=O asymmetric stretching vibration of the sodium carboxylate group (COO^-Na^+). The typical absorption at 1405 cm^{-1} corresponding to the carbonyl symmetric stretching vibration confirming the formation of the sodium carboxylate groups in the crosslinked product [41]. It was noticed that the peak intensities of C–O–C function group were obviously increased

after the reaction, which confirming as well the success of the esterification reaction. The results of FTIR analysis can validate the success of HEC crosslinking with EDTAD and formation of carboxylate anions.

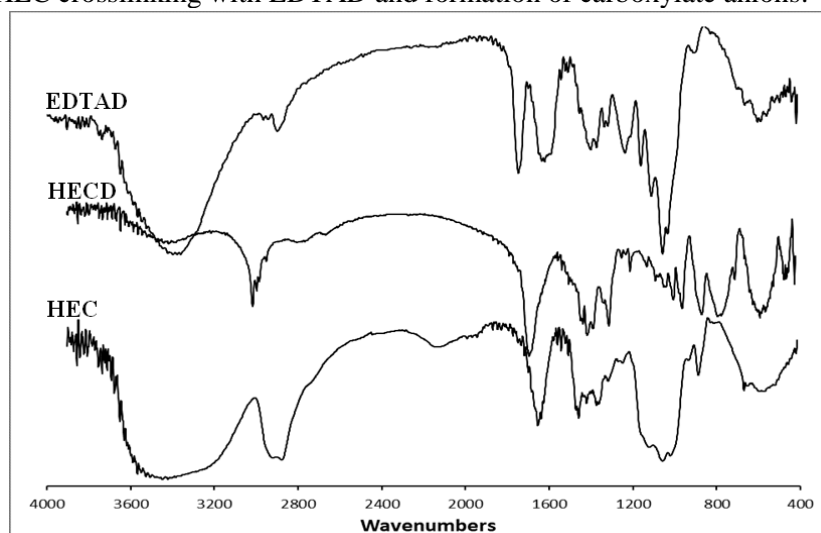


Figure 2: FTIR-ATR spectra of EDTAD, HECD and HEC

3.1.3. ^{13}C CP/MAS NMR

CP/MAS (solid-state) ^{13}C NMR spectra of unmodified HEC and HECD are shown in Fig.3. The HEC spectra showed its typical peaks. The carbon signals at 60 and 70.68 ppm were assigned to C6 and C6' (substituted) respectively. The peaks at 102.2 and 82.3 ppm are attributed to C1 and C4, respectively. The signals in the range 72.43-77.09 ppm, however, show carbon of both cellulose (C2, C3 and C5) and HEC backbone (C7, C8) [42]. In the HECD spectra, the most significant peaks indicating successful modification and sodium salt formation, respectively, appeared at 176.16 and 179.60 ppm. These peaks corresponded to the ester carbonyl (C9) and the carbonyl of COO^-Na^+ of HECD (C14), respectively [43]. The signal at 59.35 ppm was attributed to the CH_2 of EDTA; both signals at 55.55 and 52.94 ppm were assigned to the CH_2 groups of the ethyl group of EDTA on the functionalized HEC [40].

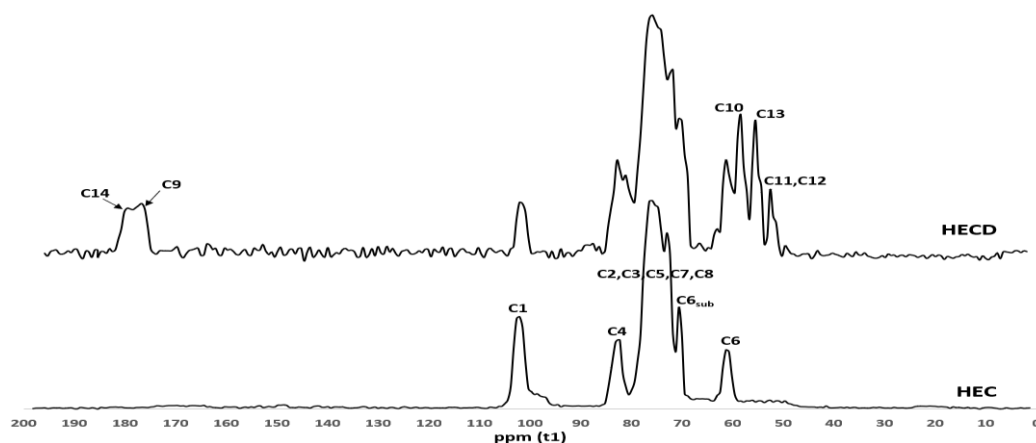


Figure 3: ^{13}C NMR CP/MAS spectra of HEC and HECD

3.1.4. TGA analysis and thermal stability

The thermal stability of HEC and HECD was determined by TGA and DTA. As shown in Fig. 4a and 4b, the loss of weight during the TG analysis of HEC can be divided into three steps. The initial weight loss (~17% for HEC) by heating the materials up to 150 °C owing to the moisture elimination with decomposition temperature (T_d) of 74 °C for

HEC [44]. The second step has T_i , T_f and T_d values of 261, 325 and 299 °C, respectively, with 28% wt was attributed to the thermal cleavage of the glucosidic units and scission of the C–O bonds [39]. The third step starts at 450 °C and represents the carbonization of the products to ash. Compared to TGA and DTA results of HEC, the Thermograms of HECD show an increase in the decomposition temperature. While the modified HEC showed three-step continuous thermal decomposition, and the weight-loss rate was obviously slowed. The weight losses of about 7wt% ($T_d = 92$ °C) correspond to the removal of the absorbed and bonded water. The weight loss of about 49 wt% (235–356 °C) can be assigned to the dehydration of saccharide rings, the breaking of ether linkage and C–N bond present in the crosslinked HEC, where there is a major weight loss [45]. However, at 50% weight loss, the decomposition temperature occurs at 310 °C for unmodified HEC and 344 °C for HECD.

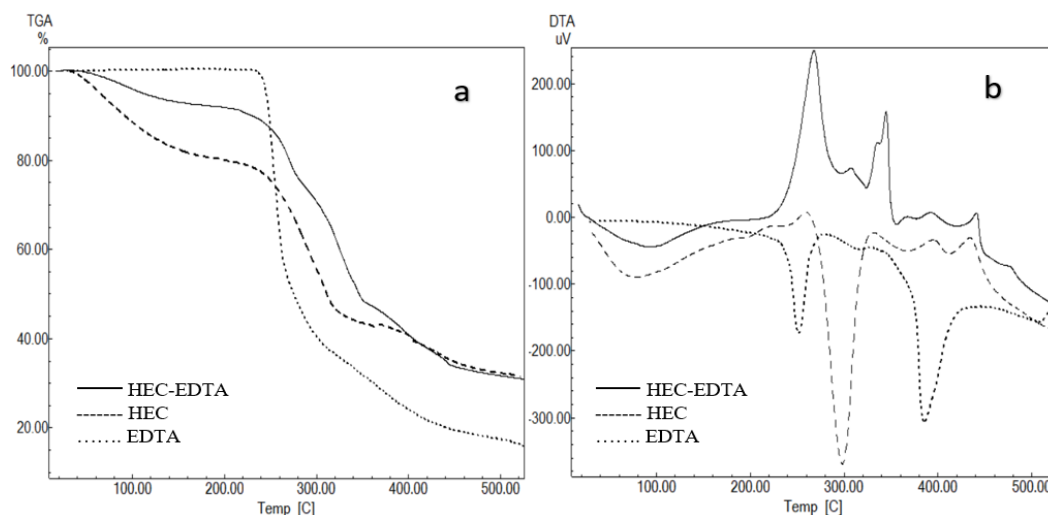


Figure 4: TGA (a) and DTA (b) spectra of HEC, EDTAD and HECD

3.1.5 Scanning electron microscopy (SEM)

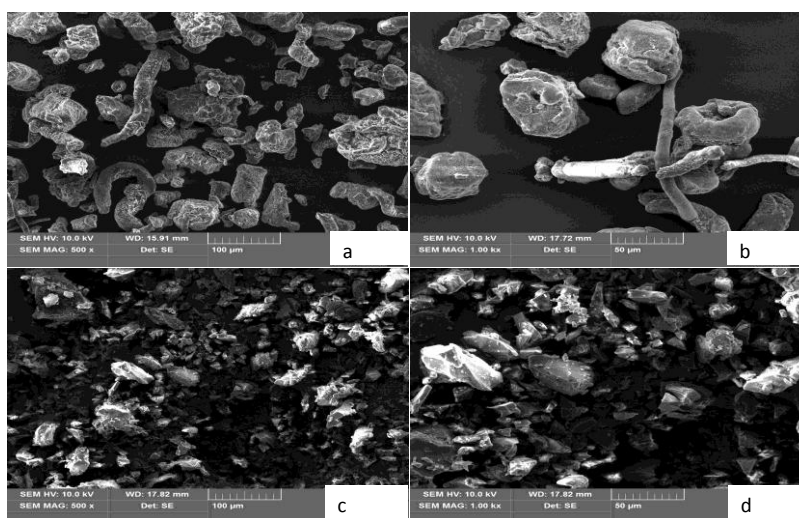


Figure 5: SEM images of HEC (a, b) and HECD (c, d)

The surface morphologies of HEC and HECD materials were recorded in Fig.5 using the electron microscopic observation. Fig.5a and b represent SEM micrographs of the initial HEC powder, showing a relatively entangled fibers and bundles with a smooth surface [46]. Fig.5c and d deal with SEM micrographs of HECD, the fibrous structure of

the material was partially destroyed and a fine powder was produced resulting in the formation of more surface interaction with the metal particles and more grain coalescence. Evidently, this situation will be helpful to pollutants absorbed. As well the modified cellulose seems to be more crystalline and its surface is more irregular and rougher than that of HEC. These results demonstrate that the hydroxyl groups located at the surface of HEC reacted with EDTA anhydride, leading to the slight destruction of the aggregates.

3.1.6. X-ray diffraction (XRD)

The X-ray diffraction patterns of HEC and HECD are shown in Fig. 6. The diffraction peak of the original HEC appears at $2\theta = 21.47^\circ$, which is assimilated to a cellulose backbone with amorphous characteristic [46, 47]. Compared with HEC, the XRD analysis of HECD shows the superposition of intensive and diffuse peaks, indicating an increasing crystallization phase and degree of crystallinity. This confirms that chemical reactions have proceeded, which resulted in a change of aggregate state.

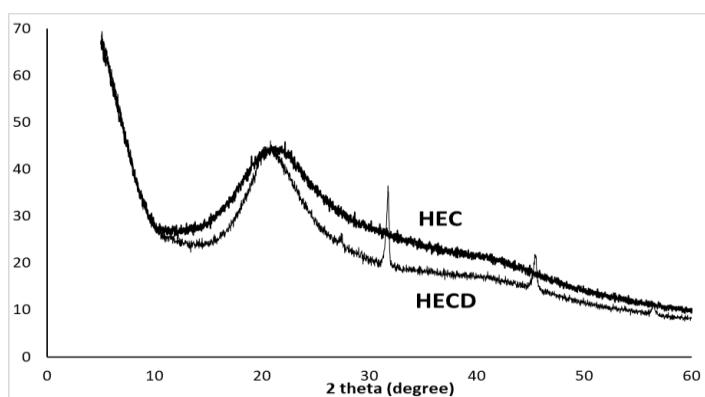


Figure 6: X-ray diffraction patterns of HEC and HECD

3.5. Adsorption capacity of HECD for metal ions

3.5.1 Effect of pH, contact time and kinetic modeling

The removal of metal ions from aqueous solutions using carboxylate functions depends strongly on the pH. It is well known that pH influences significantly the adsorption process by affecting the protonation of the surface groups where the pH desired was determined according to the total saponification of the carboxylic form to the carboxylate one [31]. To achieve the maximum extraction capacity of heavy metals by the adsorbents, knowledge of an optimum pH is important. The pH range selected to study the effect of pH on sorption was 2.0-7.0 at $T = 25^\circ\text{C}$, contact time = 30 min and optimum concentration of each metal ions and results of the effect of pH on the adsorption of Pb(II), Cu(II), Cd(II) and Zn(II) by the modified cellulose is presented in Fig. 7a. The results reveal that at low pH values ($\text{pH} < 3$), the adsorption efficiency was lowest due to the competition for adsorption sites between the metal ions and H^+ ions. As well, the carboxylate functions of material (COO^-) must be almost entirely in its protonated form (COOH), in which the predominance of carboxylic form, that cause its decrease in the number of negatively charged sites, which in turn does not favour the adsorption of positively charged metal ions [48]. Beyond pH 3, the concentration of protons decreased and the adsorbent surface charge became negative when electrostatic attraction increased between the metal ions and the adsorbent. The maximum adsorption of metals occurred at pH range from 5 to 7. At $\text{pH} > 7$ the metal ions hydrolyze in the form of hydroxides of $\text{M}(\text{OH})^+$ and $\text{M}(\text{OH})_2$. Then the optimum pH to have maximum adsorption in the case of HECD for each metal ion is between 5 and 6. The kinetic effect (contact time) on the removal of Pb(II), Cu (II), Cd (II) and Zn (II) by HECD was examined at a range time from 5 to 60 min at a pH of 6.0. The

effect of contact time on the adsorption of aqueous metal ions by HECD is shown in Fig.7b. However, during short contact times, the adsorption rate was very fast for all metal ions and the plateau was reached after about 20 min, where the fast extraction rate indicates that the adsorbent is highly suitable for the metal ions from aqueous solutions and HECD has active electron-rich atoms constituting numerous active exchange sites favouring electrostatic interactions with cationic species. The observed variation in adsorption capacity is probably due to the size of the metals, the degree of hydration, the forms of the hydroxides formed and the constant of their complexes band with the material. The pseudo-first-order and the pseudo-second-order kinetic adsorption model have been commonly used to study the kinetic behavior of adsorption processes. Since the linear equations for pseudo-first and pseudo-second kinetic orders are as follows (eq.5 and eq.6):

$$\ln(q_s - q_t) = \ln q_s - k_1 t \quad (\text{eq. 5}) \text{ Pseudo-first}$$

order

$$\frac{t}{q_t} = \frac{1}{k_2 q_s^2} - \frac{k_1 t}{q_s} \quad (\text{eq. 6}) \text{ Pseudo-second-order}$$

Where q_e and q_t are the amounts of metal ions adsorbed (mg.g^{-1}) at equilibrium and at time t , respectively, k_1 is the rate constant of the first-order adsorption in min^{-1} and k_2 ($\text{g. mg}^{-1} \text{ min}^{-1}$) is the pseudo-second-order adsorption rate constant.

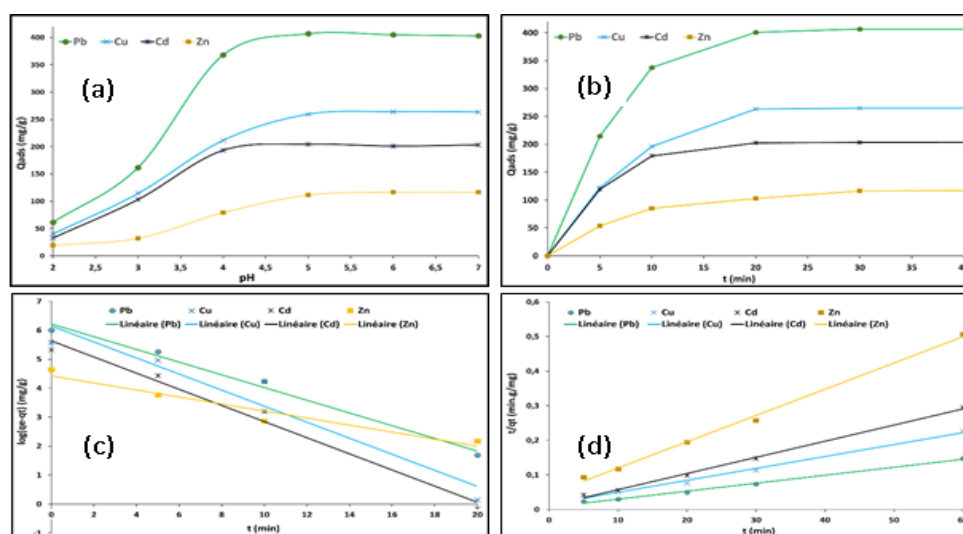


Figure 7: The adsorption of Pb (II), Cu (II), Cd (II) and Zn (II) metal ions on HECD at 25 °C (a) Effect of pH (optimum concentration, $t = 30$ min), (b) Effect of contact time (optimum concentration and $\text{pH}=6$), (c) pseudo-first-order kinetic (d) Pseudo-second order kinetic.

Model	Parameters	Pb(II)	Cu(II)	Cd(II)	Zn(II)
Experimental	$q_{e(\text{exp})} (\text{mg.g}^{-1})$	405.37	265.47	203.36	108.36
	$q_{e(\text{exp})} (\text{mmol.g}^{-1})$	001.96	004.18	001.81	001.66
Pseudo-1 ^{er} Ordre	$q_e (\text{mg.g}^{-1})$	500.85	467.64	279.95	083.58
	$K_1 (\text{min}^{-1})$	0.2194	0.2768	0.2787	0.1216
	R^2	0.9830	0.9720	0.9740	0.9720
Pseudo-2 ^{eme} Ordre	$q_e (\text{mg/g})$	416.67	277.78	212.76	126.58
	$K_2 (\text{g. mg}^{-1} \text{ min}^{-1})$	0.0007	0.0008	0.0020	0.0014
	R^2	0.9950	0.9960	0.9950	0.9930

Table 1: Kinetic parameters of the two models applied in metal ions adsorption

The results of kinetic modeling of linear pseudo-second-order model are shown in Fig.7c and d. The values of kinetic parameters are presented in Table 1. The values of the regression coefficient (R^2) show that the most appropriate model for describing the adsorption of Pb(II), Cu(II), Cd(II) and Zn(II) on HECD is the pseudo-second-order model. This is in good agreement with the literature, which indicates that the adsorption of metal ions on cellulosic substrates obeyed a pseudo-second-order kinetic model.

3.5.2. Adsorption isotherm modeling and Thermodynamic studies

The effect of the initial Pb(II), Cu(II), Cd(II) and Zn(II) concentration on the adsorption capacity was investigated by varying the initial metal ion concentration between 10 and 600 (mg.L^{-1}) on the modified hydroxyethyl cellulose (Fig.8a). The adsorption studies were accomplished at a pH of 6.0 and room temperature. Initially, the adsorption capacity of metal ions was faster, followed by a slow down to the equilibrium state, indicating the saturation of the active chelates sites. The equilibrium data isotherm analysis for heavy metal adsorption onto HECD can be mathematically expressed in terms of adsorption isotherm models. The objective is to evaluate the most appropriate correlations for equilibrium curves and then optimize the design of a sorption system. Langmuir and Freundlich isotherm models were used to describe the adsorption equilibrium. However, the Langmuir model proposes that the adsorption happens on the surface of the solid that consists of elementary sites, each of which can receive one adsorbate entity. However, the model supposes that every site is equivalent, it was also assumed that the ability of the adsorbate to get bond is independent of the fact that the neighbouring sites are occupied or not. Freundlich isotherm model, also widely used, it describes the sorption of the solute from liquid onto the solid surface. It supposes that the strongest binding sites are occupied first after that the binding strength decreases once the degree of site occupation increase.

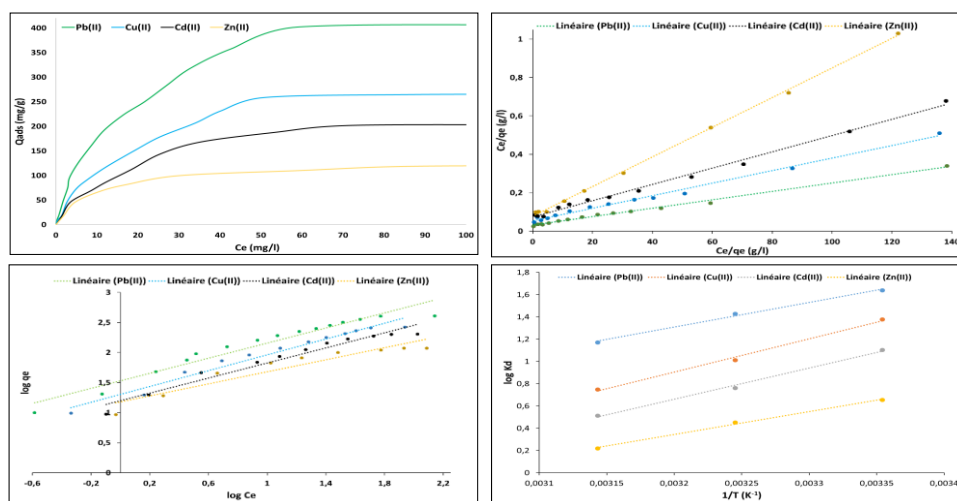


Figure 8: Adsorption isotherms and Thermodynamic parameters, (a) Effect of the initial concentration of metal ions, (b) Langmuir adsorption modeling, (c) Freundlich adsorption modelling, (d) Temperature effect.

Freundlich model assumes monolayer sorption and proposes a heterogeneous energetic distribution of active sites, and/or interactions between adsorbed entities. Langmuir and Freundlich models are given as follows, respectively:

$$q_e = \frac{qbC_e}{1+bC_e} \quad (\text{eq. 7})$$

$$q_e = K_e C_e \quad (\text{eq. 8})$$

Equations 7 and 8 can be linearized as follows, respectively:

$$\frac{C_e}{q_e} = \frac{C_e}{q} + \frac{1}{qK_L} \quad (eq. 9)$$

$$\log q_e = \log K_F + \frac{1}{n} \log C_e \quad (eq.10)$$

Where q_e is the quantity of the solute adsorbed (mg.g^{-1}), C_e is the equilibrium concentration ion in the solution (mg.L^{-1}), q (mg.g^{-1}) is the maximum adsorption capacity. K_L (L.mg^{-1}) is the Langmuir constant related to the free adsorption energy, K_F (mg.g^{-1}) is Freundlich constants related to the adsorption capacity and n is Freundlich constants to the adsorption intensity.

The isotherm models' parameters are computed from the slopes and intercepts of straight lines representing the interaction of HECD with different metal ions (Fig. 8b and c). These calculated values are shown in Table 2.

Table 2: Langmuir and Freundlich adsorption isotherms parameters

Metal ion	Langmuir			Freundlich		
	q (mg.g^{-1})	K_L (L.mg^{-1})	R^2	K_F (mg.g^{-1})	n	R^2
Pb(II)	434.78	0.071	0.994	36.52	1.63	0.96
Cu(II)	294.64	0.064	0.996	20.46	1.53	0.94
Cd(II)	233.10	0.059	0.997	15.90	1.59	0.95
Zn(II)	129.95	0.090	0.997	14.01	1.93	0.89

The comparison of correlation coefficients values (R^2) of the linearized form of both Langmuir and Freundlich models shows that the Langmuir model yields a better fit for the experimental adsorption equilibrium data with R^2 values are ≥ 0.994 , indicating a very good mathematical fit and the most suitable isotherm to describe the equilibrium data for the metal adsorption process of Pb (II), Cu (II), Cd (II) and Zn (II) onto the crosslinked hydroxyethyl cellulose.

Alternatively, the influence of temperature is an important parameter influencing the adsorption process. Though, it was studied in the range 25- 45°C of temperature. The experiments have been achieved under the same optimum conditions of concentrations, pH and contact time. The thermodynamic parameters offer detailed information on characteristic energetic changes that are associated with adsorption. The thermodynamic parameters of adsorption including the free energy change $\Delta G^\circ = \Delta H^\circ - T\Delta S^\circ = -RT \ln K_c$, the enthalpy change ΔH_0 and the entropy change ΔS_0 were determined, using the equations 10, 11 and 12:

$$\Delta G^\circ = \Delta H^\circ - T\Delta S^\circ = -RT \ln K_c \quad (eq. 11)$$

$$K_c = \frac{q_e}{C_e} \quad (eq. 12)$$

$$\ln K_c = -\frac{\Delta H^\circ}{R} \frac{1}{T} + \frac{\Delta S^\circ}{R} \quad (eq. 13)$$

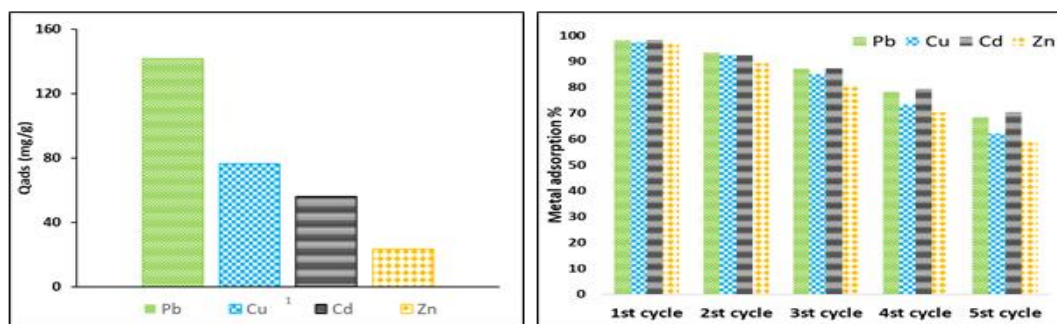
Where K_c is the thermodynamic equilibrium constant, R is the general gas constant and T is the absolute temperature K. The enthalpy change ΔH_0 and the entropy change ΔS_0 , were obtained from the slope and intercept of the plot of $\ln(K_c)$ against $1/T$ (Fig. 8d). The values of thermodynamic parameters are calculated and given in Table3. The results show that the $\Delta G^\circ = \Delta H^\circ - T\Delta S^\circ = -RT \ln K_c$ values are negative at all studied temperatures, indicating the spontaneous nature of the adsorption process of metal ions onto the crosslinked material. The positive ΔH° value designates the endothermic nature of the adsorption process. Moreover, the positive ΔS° reveals the decrease in randomness at the solid-solution interface through the adsorption processes of metal ions onto HECD.

Table 3: Thermodynamic parameters of the metal ions removal process

Metal ions	R ²	ΔH° (kJ.mol ⁻¹)	ΔS° (J.K ⁻¹ .mol ⁻¹)	T (K)	ΔG° (kJ.mol ⁻¹)
Pb(II)	0,995	-24.91	-69.75	298.15	-4.110
				308.15	-3.412
				318.15	-2.714
Cu(II)	0,995	-23.16	-66.30	298.15	-3.394
				308.15	-2.731
				318.15	-2.068
Cd(II)	0,996	-23.28	-68.67	298.15	-2.802
				308.15	-2.116
				318.15	-1.429
Zn(II)	0,994	-17.09	-51.55	298.15	-1.717
				308.15	-1.202
				318.15	-0.686

3.5.3. The metallic selectivity and Regenerability of material (HECD)

A solution containing Pb(II), Cu(II), Cd(II) and Zn(II) was agitated with HECD to study the competitive removal of metal ions under optimal conditions and the results are presented in Fig.9a. HECD showed adsorption capacities of 141.65 mg/g (0,683 mmol/g), 76.4 mg/g (1,2 mmol/g), 56.31 mg/g (0,5 mmol/g) and 23.37mg/g (0,36 mmol/g) for Pb(II), Cu(II), Cd(II) and Zn(II), respectively. Adsorption capacity value of each metal ions in the mixture of metal ions was less than its value in single metal ions solution. This is due to the fact that in a single metal system there is no competition between different metal ions for sorption sites on the surface of the sorbent. However, the material shows a remarkable selectivity to Cu(II) with an extraction capacity of about 76.4 mg/g (1,2 mmol/g). Furthermore, the stability of the adsorbent was studied by regeneration experiments. This study of regeneration and reuse of the adsorbent is extremely important since it has a direct influence on the economic feasibility of the adsorbent material. In this context, the sorption-desorption studies of the metal ions were carried out over five successive cycles. The sample was easily regenerated by soaking the sample in 2N HCl for 15 minutes. Fig. 9b shows that total decrease in term of percentage uptake was 31.5, 37.8, 29.4 and 40.6% for Pb(II), Cu(II), Cd(II) and Zn(II), respectively after five cycles. During the regeneration, the adsorption efficiency was radically affected by the regeneration process in acidic medium. These results show a high stability and a good recyclability of adsorbents suggesting the repeated use of sorbent before need to be replaced.

**Figure 9:** Adsorption selectivity of HECD (a) and Regenerability study using nitric acid medium (b)

4. Conclusion

Through a quick, efficient, and inexpensive methodology, we carried out the homogeneous esterification crosslinking of HEC by EDTA dianhydride. In addition, crosslinking and grafting of HEC was occurred by the formation of diester and monoester linkages. This produced material was found to be an efficient adsorbent in simulated decontamination solutions and showed good adsorption properties. This study showed that HECD is an effective adsorbent for removal of heavy metal ions from aqueous solutions with adsorption capacities values of 405.37, 265.47, 203.36 and 108.36 mg/g for Pb (II), Cu (II), Cd (II) and Zn (II), respectively. The molar adsorption capacity values shown the following adsorption order, Cu(II) > Pb(II) > Cd(II) > Zn(II), whose maximum adsorption capacities were found to be 1.96, 4.18, 1.81 and 1.66 mmol/g. This work also shows that the adsorption process is best described by the Langmuir isotherm model, the nature of the adsorption process was exothermic and spontaneous, and finally that the adsorption kinetics were represented by a pseudo-second-order model. The adsorption results suggest that this modified hydroxyethyl cellulose could be utilized for the removal of divalent cations from an aqueous solution contaminated with heavy metals.

References

- [1] V. Gupta, I. Ali, Water treatment for inorganic pollutants by adsorption technology, *Environ. Water.* 29 (2013).
- [2] A.P. Lim, A.Z. Aris, A review on economically adsorbents on heavy metals removal in water and wastewater, *Reviews in Environmental Science and Bio/Technology* 13 (2014) 163-181.
- [3] X. Ma, Y. Li, Z. Ye, L. Yang, L. Zhou, L. Wang, Novel chelating resin with cyanoguanidine group: useful recyclable materials for Hg (II) removal in aqueous environment, *J. Hazard. Mater.* 185 (2011) 1348-1354.
- [4] J. Glover-Kerkvliet, Environmental assault on immunity, 1995.
- [5] W.R. García-Niño, J. Pedraza-Chaverri, Protective effect of curcumin against heavy metals-induced liver damage, *Food Chem. Toxicol.* 69 (2014) 182-201.
- [6] P.O. Boamah, Y. Huang, M. Hua, Q. Zhang, J. Wu, J. Onumah, L.K. Sam-Amoah, P.O. Boamah, Sorption of heavy metal ions onto carboxylate chitosan derivatives—a mini-review, *Ecotoxicol. Environ. Saf.* 116 (2015) 113-120.
- [7] N.S.A. Mutamim, Z.Z. Noor, M.A.A. Hassan, G. Olsson, Application of membrane bioreactor technology in treating high strength industrial wastewater: a performance review, *Desalination* 305 (2012) 1-11.
- [8] M. Visa, Synthesis and characterization of new zeolite materials obtained from fly ash for heavy metals removal in advanced wastewater treatment, *Powder Technol.* 294 (2016) 338-347.
- [9] D. Ghernaout, A.I. Al-Ghonamy, A. Boucherit, B. Ghernaout, M.W. Naceur, N.A. Messaoudene, M. Aichouni, A.A. Mahjoubi, N.A. Elboughdiri, Brownian motion and coagulation process, *Am. J. Environ. Prot* 4 (2015) 1-15.
- [10] F. Renault, B. Sancey, P.-M. Badot, G. Crini, Chitosan for coagulation/flocculation processes—an eco-friendly approach, *European Polymer Journal* 45 (2009) 1337-1348.
- [11] Z. Hubicki, D. Kołodyńska, Selective removal of heavy metal ions from waters and waste waters using ion exchange methods, *Ion Exchange Technologies*, IntechOpen2012.
- [12] B. An, Q. Liang, D. Zhao, Removal of arsenic (V) from spent ion exchange brine using a new class of starch-bridged magnetite nanoparticles, *Water Res.* 45 (2011) 1961-1972.
- [13] P.-S. Keng, S.-L. Lee, S.-T. Ha, Y.-T. Hung, S.-T. Ong, Cheap materials to clean heavy metal polluted waters, *Green Materials for Energy, Products and Depollution*, Springer2013, 335-414.
- [14] I. Aguayo-Villarreal, A. Bonilla-Petriciolet, R. Muñoz-Valencia, Preparation of activated carbons from pecan nutshell and their application in the antagonistic adsorption of heavy metal ions, *J. Mol. Liq.* 230 (2017) 686-695.
- [15] M. Hossain, H. Ngo, W. Guo, T. Nguyen, Palm oil fruit shells as biosorbent for copper removal from water and *Mor. J. Chem.* 8 N°1 (2020) 332-346

wastewater: experiments and sorption models, *Bioresour. Technol.* 113 (2012) 97-101.

[16] R. Mallampati, L. Xuanjun, A. Adin, S. Valiyaveetil, Fruit peels as efficient renewable adsorbents for removal of dissolved heavy metals and dyes from water, *ACS Sustainable Chemistry & Engineering* 3 (2015) 1117-1124.

[17] K. Chauhan, G.S. Chauhan, J.-H. Ahn, Synthesis and characterization of novel guar gum hydrogels and their use as Cu²⁺ sorbents, *Bioresour. Technol.* 100 (2009) 3599-3603.

[18] B. Anna, M. Kleopas, S. Constantine, F. Anestis, B. Maria, Adsorption of Cd (II), Cu (II), Ni (II) and Pb (II) onto natural bentonite: study in mono-and multi-metal systems, *Environmental Earth Sciences* 73 (2015) 5435-5444.

[19] L. Yan, S. Li, H. Yu, R. Shan, B. Du, T. Liu, Facile solvothermal synthesis of Fe₃O₄/bentonite for efficient removal of heavy metals from aqueous solution, *Powder Technol.* 301 (2016) 632-640.

[20] J. Wang, C. Chen, Chitosan-based biosorbents: modification and application for biosorption of heavy metals and radionuclides, *Bioresour. Technol.* 160 (2014) 129-141.

[21] F.-L. Mi, S.-J. Wu, F.-M. Lin, Adsorption of copper (II) ions by a chitosan-oxalate complex biosorbent, *International journal of biological macromolecules* 72 (2015) 136-144.

[22] C. Barquilha, E. Cossich, C. Tavares, E. Silva, Biosorption of nickel (II) and copper (II) ions in batch and fixed-bed columns by free and immobilized marine algae *Sargassum* sp, *Journal of Cleaner Production* 150 (2017) 58-64.

[23] L. Zhang, Y. Zeng, Z. Cheng, Removal of heavy metal ions using chitosan and modified chitosan: A review, *J. Mol. Liq.* 214 (2016) 175-191.

[24] M. Li, Z. Zhang, R. Li, J.J. Wang, A. Ali, Removal of Pb (II) and Cd (II) ions from aqueous solution by thiosemicarbazide modified chitosan, *International journal of biological macromolecules* 86 (2016) 876-884.

[25] A. Benettayeb, E. Guibal, A. Morsli, R. Kessas, Chemical modification of alginate for enhanced sorption of Cd (II), Cu (II) and Pb (II), *Chem. Eng. J.* 316 (2017) 704-714.

[26] I. Siró, D. Plackett, Microfibrillated cellulose and new nanocomposite materials: a review, *Cellulose* 17 (2010) 459-494.

[27] S. Ummartyotin, H. Manuspiya, A critical review on cellulose: from fundamental to an approach on sensor technology, *Renewable and Sustainable Energy Reviews* 41 (2015) 402-412.

[28] S. Hokkanen, E. Repo, M. Sillanpää, Removal of heavy metals from aqueous solutions by succinic anhydride modified mercerized nanocellulose, *Chemical engineering journal* 223 (2013) 40-47.

[29] T. Hajeeth, K. Vijayalakshmi, T. Gomathi, P. Sudha, Removal of Cu (II) and Ni (II) using cellulose extracted from sisal fiber and cellulose-g-acrylic acid copolymer, *International journal of biological macromolecules* 62 (2013) 60.

[30] O.K. Júnior, L.V.A. Gurgel, R.P. de Freitas, L.F. Gil, Adsorption of Cu(II), Cd(II), and Pb(II) from aqueous single metal solutions by mercerized cellulose and mercerized sugarcane bagasse chemically modified with EDTA dianhydride (EDTAD), *Carbohydrate Polymers* 77 (2009) 643, <http://dx.doi.org/10.1016/j.carbpol.2009.02.016>.

[31] I. Jilal, S. El Barkany, Z. Bahari, O. Sundman, A. El Idrissi, M. Abou-Salama, A. Romane, C. Zannagui, H. Amhamdi, New quaternized cellulose based on hydroxyethyl cellulose (HEC) grafted EDTA: Synthesis, characterization and application for Pb (II) and Cu (II) removal, *Carbohydr. Polym.* 180 (2018) 156-167.

[32] D. Chattopadhyay, S. Banerjee, D. Chakravorty, B. Mandal, Ethyl (hydroxyethyl) cellulose stabilized polyaniline dispersions and destabilized nanoparticles therefrom, *Langmuir* 14 (1998) 1544-1547.

[33] Z. Hu, H.S. Marway, H. Kasem, R. Pelton, E.D. Cranston, Dried and redispersible cellulose nanocrystal Pickering emulsions, *ACS Macro Letters* 5 (2016) 185-189.

[34] E. Abdel-Halim, Preparation and characterization of poly (acrylic acid)-hydroxyethyl cellulose graft copolymer, *Carbohydr. Polym.* 90 (2012) 930-936.

[35] Q. Zhou, E. Malm, H. Nilsson, P.T. Larsson, T. Iversen, L.A. Berglund, V. Bulone, Nanostructured biocomposites
Mor. J. Chem. 8 N°1 (2020) 332-346

based on bacterial cellulosic nanofibers compartmentalized by a soft hydroxyethylcellulose matrix coating, *Soft Matter* 5 (2009) 4124-4130.

[36] Q. Zhou, L. Zhang, M. Li, X. Wu, G. Cheng, Homogeneous hydroxyethylation of cellulose in NaOH/urea aqueous solution, *Polym. Bull.* 53 (2005) 243-248.

[37] L. Tanghe, L. Genung, J.W. Mench, Determination of acetyl content and degree of substitution of cellulose acetate, *Methods in carbohydrate chemistry* 3 (1963) e203.

[38] W. Li, A. Jin, C. Liu, R. Sun, A. Zhang, J. Kennedy, Homogeneous modification of cellulose with succinic anhydride in ionic liquid using 4-dimethylaminopyridine as a catalyst, *Carbohydrate Polymers* 78 (2009) 389-395.

[39] A. El Idrissi, S. El Barkany, H. Amhamdi, A.K. Maaroufi, Synthesis and characterization of the new cellulose derivative films based on the hydroxyethyl cellulose prepared from esparto "stipa tenacissima" cellulose of Eastern Morocco. II. Esterification with acyl chlorides in a homogeneous medium, *J. Appl. Polym. Sci.* 127 (2013) 3633-3644.

[40] A. Abbas, M.A. Hussain, M. Sher, M.I. Irfan, M.N. Tahir, W. Tremel, S.Z. Hussain, I. Hussain, Design, characterization and evaluation of hydroxyethylcellulose based novel regenerable supersorbent for heavy metal ions uptake and competitive adsorption, *International journal of biological macromolecules* 102 (2017) 170-180.

[41] W. Wang, J. Wang, Y. Kang, A. Wang, Synthesis, swelling and responsive properties of a new composite hydrogel based on hydroxyethyl cellulose and medicinal stone, *Composites Part B: Engineering* 42 (2011) 809-818.

[42] L. Zhang, J. Zhou, L. Zhang, Synthesis and Fluorescent Properties of Carbazole- Substituted Hydroxyethylcelluloses, *Macromol. Chem. Phys.* 213 (2012) 57-63.

[43] A. Labidi, A.M. Salaberria, S.C. Fernandes, J. Labidi, M. Abderrabba, Adsorption of copper on chitin-based materials: Kinetic and thermodynamic studies, *Journal of the taiwan institute of chemical engineers* 65 (2016) 140-148.

[44] E. Abderahmane, S. El Barkany, A. Hassan, M. Abdel- Karim, Synthesis and characterization of the new cellulose derivative films based on the hydroxyethyl cellulose prepared from "Stipa Tenacissima" cellulose of Eastern Morocco. I. Solubility study, *J. Appl. Polym. Sci.* 122 (2011) 2952-2965.

[45] H. Ge, S. Huang, Microwave preparation and adsorption properties of EDTA- modified cross- linked chitosan, *J. Appl. Polym. Sci.* 115 (2010) 514-519.

[46] R. Chen, C. Yi, H. Wu, S. Guo, Degradation kinetics and molecular structure development of hydroxyethyl cellulose under the solid state mechanochemical treatment, *Carbohydr. Polym.* 81 (2010) 188-195.

[47] M. Trivedi, G. Nayak, S. Patil, R.M. Tallapragada, R.K. Mishra, Influence of biofield treatment on physicochemical properties of hydroxyethyl cellulose and hydroxypropyl cellulose, *Molecular Pharmaceutics & Organic Process Research* 3 (2015).

[48] M. Iqbal, A. Saeed, I. Kalim, Characterization of adsorptive capacity and investigation of mechanism of Cu²⁺, Ni²⁺ and Zn²⁺ adsorption on mango peel waste from constituted metal solution and genuine electroplating effluent, *Separation Science and Technology* 44 (2009) 3779.